The Canadian Mineralogist
Vol. 42, pp. 1047-1056 (2004)

CHROMATE ALUMINATE SODALITE, $Ca_8[Al_{12}O_{24}](CrO_4)_2$: PHASE TRANSITIONS AND HIGH-TEMPERATURE STRUCTURAL EVOLUTION OF THE CUBIC PHASE

SYTLE M. ANTAO[§]

Mineral Physics Institute & Department of Geosciences, State University of New York, Stony Brook, New York 11794-2100, U.S.A.

ISHMAEL HASSAN

Department of Chemistry, University of the West Indies, Mona, Kingston 7, Jamaica

JOHN B. PARISE

Mineral Physics Institute & Department of Geosciences, State University of New York, Stony Brook, New York 11794-2100, U.S.A.

ABSTRACT

The structural behavior of a chromate aluminate sodalite, $Ca_8[Al_{12}O_{24}](CrO_4)_2$, at room pressure and on heating from 463 to 982°C was determined by using *in situ* synchrotron X-ray powder-diffraction data [$\lambda = 0.91997(4)$ Å] and Rietveld refinements. The sample was heated at a rate of about 9.5°C/min., and X-ray traces were collected at intervals of about 17°C. The structure at 463°C is a modulated cubic phase, whereas above 512°C, the structure is cubic with space group $I\bar{4}3m$. The *a* parameter increases linearly from 512 to 982°C, and the percent change in volume is 0.9(1)%. Between 463 and 982°C, the Al–O distance is nearly constant, the angle of rotation of the AlO_4 tetrahedron, φ_{Al}, decreases by 0.6° and simultaneously, the Al–O–Al bridging angle increases by 0.8(2)°. Between 463 to 982°C, the Ca–O distances are nearly constant. The Ca atom is located nearly in the plane of the three O' framework atoms, so movement of the Ca atom out of this plane will cause longer Ca–O' bonds instead of shorter bonds that occur when the Ca atom is migrating toward this plane. The highly charged $[Ca_4{\bullet}CrO_4]^{6+}$ clusters bond strongly to the framework oxygen atoms, which limits the rotation of the framework AlO_4 tetrahedra; as a result, the expansion of the structure is small. We evaluate the differences between the thermal behavior of chromate aluminate sodalite and that of other structurally related phases (*e.g.*, sodalite and danalite).

Keywords: chromate aluminate sodalite, phase transitions, high-temperature structures, synchrotron radiation, Rietveld refinement.

SOMMAIRE

Nous avons déterminé le comportement structural d'un composé synthétique dérivé de la sodalite, et ayant la composition $Ca_8[Al_{12}O_{24}](CrO_4)_2$, à pression ambiante et au cours d'un chauffage entre 463 à 982°C, en utilisant la diffraction X *in situ* sur poudre, avec rayonnement synchrotron [$\lambda = 0.91997(4)$ Å] et la méthode de Rietveld. L'échantillon est chauffé à un taux d'environ 9.5°C/min., et les tracés de diffraction X ont été prélevés à un intervalle d'environ 17°C. La structure à 463°C est cubique et modulée, tandis qu'au delà de 512°C, elle est cubique, groupe spatial $I\bar{4}3m$. Le paramètre *a* augmente de façon linéaire entre 512 et 982°C, et le volume augmente de 0.9(1)%. Entre 463 et 982°C, la distance Al–O est presque constante, et l'angle de rotation φ_{Al} des tétraèdres AlO_4 diminue de 0.6°; de façon simultanée, l'angle du pont Al–O–Al augmente de 0.8(2)°. Entre 463 et 982°C, les distances Ca–O sont presque constantes. L'atome Ca est situé presque dans le plan des trois atomes O' de la trame, de sorte que le mouvement de cet atome au delà de ce plan devrait causer un allongement des liaisons Ca–O', plutôt que des liaisons plus courtes qui sont attendues si l'atome de Ca migre dans la direction de ce plan. Les groupements $[Ca_4{\bullet}CrO_4]^{6+}$, possédant une charge élevée, sont fortement liés aux atomes d'oxygène de la trame, ce qui limite la rotation des tétraèdres de AlO_4 de la trame. L'expansion de la structure est donc limitée. Nous évaluons les différences entre le comportement thermique de ce composé de sodalite à aluminate et chromate et celui d'autres composés structuralement semblables, par exemple, sodalite et danalite.

(Traduit par la Rédaction)

Mots-clés: sodalite à chromate et aluminate, transitions de phases, structures à température élevée, rayonnement synchrotron, affinement de Rietveld.

§ *E-mail address*: sytle.antao@stonybrook.edu

Introduction

We have studied a synthetic sodalite-group compound, $Ca_8[Al_{12}O_{24}](CrO_4)_2$, that contains $[Ca_4{\bullet}CrO_4]^{6+}$ clusters in the sodalite "cage". This material, which we will call "chromate aluminate sodalite", undergoes several polymorphic phase-transitions on heating. The various polymorphs were observed using TEM (transmission electron microscopy) by Hassan (1996a–e). The TEM results reveal the occurrence of an orthorhombic, a tetragonal, a modulated cubic phase, and a cubic phase. In addition, twinning and periodic antiphase-domain boundaries were observed. The modulated cubic phase contains satellite reflections that are similar to those that occur in aluminosilicate sodalite-group minerals (*e.g.*, nosean, haüyne, and lazurite), which contain SO_4^{2-} as the dominant interstitial anion (*e.g.*, Saalfeld 1961, Taylor 1968, Schulz 1970, Hassan *et al.* 1985). The satellite reflections indicate that the structures of sulfatic sodalite-group phases are incommensurately modulated. As a result, these minerals also were studied by TEM (*e.g.*, Morimoto 1978, Tsuchiya & Takéuchi 1985, Hassan & Buseck 1989a, b, Hassan 2000). The chromate aluminate sodalite specimen used in this study also contains satellite reflections (*e.g.*, Hassan 1996d).

The thermal expansion of sodalite and structurally related materials was studied by high-temperature X-ray powder diffraction (*e.g.*, Taylor 1968, Henderson & Taylor 1978); no detailed high-temperature structural work was done on $Ca_8[Al_{12}O_{24}](CrO_4)_2$, however. The present study was carried out to determine the polymorphic phase-transitions exhibited by $Ca_8[Al_{12}O_{24}](CrO_4)_2$ and the structural behavior of one polymorph, the cubic form, to 982°C using *in situ* synchrotron X-ray powder-diffraction data and Rietveld structure refinements. Detailed results on the structures of the tetragonal and orthorhombic phases will be published separately. X-ray powder-diffraction data eliminates the effect of twinning and periodic antiphase boundaries that occur in single crystals on the TEM scale. The thermal expansion of cubic chromate aluminate sodalite is discussed in terms of the observed structural changes and the geometrical model of Hassan & Grundy (1984). This study provides further insights into the structural behavior of sodalite-group minerals in general, several of which were recently determined (Hassan *et al.* 2004a, b, Antao *et al.* 2003, 2004).

Background Information

The structure of cubic chromate aluminate sodalite (space group $I\bar{4}3m$) was refined by Melzer & Depmeier (1996). The framework structure is characterized by four-membered rings in the faces of the unit cell, and these rings are linked to form six-membered rings about the corners of the unit cell (Fig. 1). These rings consist only of Al atoms instead of Al and Si atoms as in sodalite proper. The cages in aluminate sodalite can accommodate a variety of interstitial cations and anions by cooperative rotation (angle φ_{Al}) of the AlO_4 tetrahedra from their positions in a fully expanded state, where φ_{Al} is zero (Fig. 1). In chromate aluminate sodalite, the CrO_4^{2-} group occurs as the interstitial anion, and the interstitial cations are Ca^{2+}. These Ca^{2+} cations occupy 8(c) positions on the body diagonals of the cubic cell. The CrO_4^{2-} groups may be positionally disordered about the center and corners of the cubic cell. The various patterns of ordering for the CrO_4^{2-} groups give rise to several polymorphs. The molybdate analogue of the aluminate sodalite, $Ca_8[Al_{12}O_{24}](MoO_4)_2$, also displays several polymorphs, and their structures were characterized by Van Smaalen *et al.* (1997). The structures of other aluminate sodalites also are available, for example, $Ca_8[Al_{12}O_{24}](WO_4)_2$ and $Sr_8[Al_{12}O_{24}](CrO_4)_2$ (Melzer & Depmeier 1996).

Experimental Methods

The chromate aluminate sodalite under investigation was crushed to a powder using an agate mortar and pestle. High-temperature synchrotron powder X-ray-diffraction (XRD) experiments were performed at beam-line X7B of the National Synchrotron Light Source at Brookhaven National Laboratory. The sample was loaded in a silica capillary (diameter = 0.5 mm, open to air at one end) and was oscillated during the experiment over an angle of 10°. The high-temperature XRD data were collected using *in situ* synchrotron

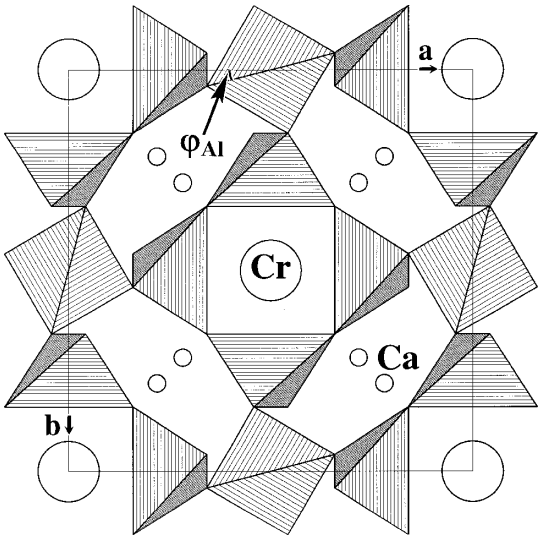

FIG. 1. [001] projection of the chromate aluminate sodalite structure at 982°C, showing the lower half of the unit-cell. The angle of rotation of an AlO_4 tetrahedron is indicated by φ_{Al}.

radiation [λ = 0.91997(4) Å] at room pressure and from 26 to 982°C. The sample was heated at a rate of about 9.5°C/min. using a horseshoe-shaped heater and controlled using a thermocouple element near the capillary. The diffraction data were collected in regular intervals of about 17°C. The data were collected to a maximum 2θ of about 50° [(sinθ/λ) < 0.46 $Å^{-1}$]. An imaging plate (IP) detector (Mar345, 2300 × 2300 pixels) mounted perpendicular to the beam path was used to collect full-circle Debye–Scherrer rings with an exposure time of 10 s. In a separate experiment, a LaB_6 standard was used to determine the sample-to-detector distance, tilt angle, wavelength, and tilting angle of the IP. The diffraction patterns recorded on the IP were integrated using the Fit2d program (Hammersley 1996).

Rietveld Refinements of the Structure

Several XRD traces were selected at regular temperature intervals for treatment with the Rietveld method, *GSAS,* and *EXPGUI* programs (Larson & Von Dreele 2000, Toby 2001). For the cubic high-temperature structure, the starting coordinates of the atoms, cell parameter, isotropic displacement parameters, and space group, $I\bar{4}3m$, were those of Melzer & Depmeier (1996). Chromate aluminate sodalite displays $I\bar{4}3m$ symmetry only at high temperatures because this material shows satellite reflections at lower temperatures (less than 512°C) that indicate a lower symmetry than cubic.

In the initial stage, the background was fitted by using the Chebyschev analytical function with 24 coefficients, and the profiles were fitted using the pseudo-Voigt function and an asymmetry correction term (GV, GW, LY, and asym). The zero-shift was set to zero at all temperatures. A full-matrix least-squares refinement, carried out by varying a scale factor, the cell parameter, atom coordinates, and isotropic displacement parameters, converged quickly. Isotropic displacement parameters were used for all the atoms; the atoms of the CrO_4^{2-} group were constrained to have equal isotropic displacement parameter ($U_{Cr} = U_{OCr}$) because the CrO_4^{2-} group is rigid. The ideal chemical formula for chromate aluminate sodalite was used to constrain the site-occupancy factors (*sof*) of the atoms in the structural model. Refinement of the *sof* for the interstitial atoms (Ca, Cr, and O_{Cr}) indicates that the chemical formula for chromate aluminate sodalite is appropriate; as a result, the *sof* for all the atoms were set to be invariable. At this stage, all the refinements at different temperatures seemed to be good, but the intensities for a few reflections did not match, indicating that the powdered sample contained some preferred orientations. Therefore, preferred orientation was taken into account by using the preferred orientation correction based on spherical harmonics (20 terms; texture index < 2.75), and this resulted in a considerable improvement in the refinement statistics. Initially, the orientation correction was correlated with the background terms, so the refinements were carried out by switching off the functions for orientation and background, alternatively. However, the final refinement was carried out by refining both the orientation and background functions simultaneously.

Finally, the background (24 terms), preferred orientation (20 terms), profile parameters (four terms), a scale factor, and structural parameters (10 variables) were also allowed to vary, and the refinement proceeded to convergence. The total number of variables was 59 at the end of the refinement, and the number of observed reflections was 48. The number of observations (data points) was about 2115. Synchrotron powder XRD traces are shown in Figures 2 and 3, as examples. The cell parameters and the Rietveld structure-refinement statistics at various temperatures are listed in Table 1. The atom coordinates and isotropic displacement parameters are given in Table 2, and selected bond-distances and angles are listed in Table 3.

Results and Discussion

Satellite reflections and phase transitions in chromate aluminate sodalite

Satellite reflections occur in the chromate aluminate sodalite sample used in this study. Such reflections are easily observed in selected-area electron diffraction (SAED) patterns (Hassan 1996d). In the synchrotron XRD traces, several weak satellite reflections are observed, and they indicate a variety of space groups and the presence of phase transitions (Figs. 2a, b). On the basis of observed XRD traces and structure refinements, five structural transitions are observed, and they are

TABLE 1. CUBIC CHROMATE ALUMINATE SODALITE: RIETVELD REFINEMENT* AND UNIT-CELL PARAMETERS AT VARIOUS TEMPERATURES

T (°C)	*a* (Å)	R_p	R_{wp}	Exp. R_{wp}	R_F^2	χ^2
463	9.22351(5)	0.0155	0.0219	0.0202	0.0274	1.196
512	9.22293(6)	0.0165	0.0230	0.0203	0.0270	1.306
561	9.22621(5)	0.0155	0.0222	0.0203	0.0264	1.222
626	9.23004(5)	0.0147	0.0214	0.0204	0.0345	1.125
674	9.23261(5)	0.0155	0.0222	0.0204	0.0232	1.209
723	9.23537(6)	0.0152	0.0224	0.0204	0.0229	1.229
771	9.23791(5)	0.0150	0.0217	0.0205	0.0224	1.136
820	9.24124(5)	0.0150	0.0215	0.0206	0.0359	1.105
869	9.24421(5)	0.0151	0.0216	0.0206	0.0271	1.117
901	9.24569(5)	0.0149	0.0212	0.0206	0.0256	1.072
933	9.24675(6)	0.0158	0.0228	0.0206	0.0266	1.242
982	9.25191(6)	0.0156	0.0225	0.0207	0.0262	1.204

* R_p = pattern R factor = $\{\Sigma|(I_o - I_c)|\} / \Sigma I_o$; R_{wp} = weighted pattern R factor = $\{\Sigma[w(I_o - I_c)^2] / \Sigma[wI^2_o]\}^{1/2}$, where I_o = observed intensity, I_c = calculated intensity, and $w = 1/I_o$; R_p and R_{wp} are the fitted values obtained without background subtraction; Exp R_{wp} = expected value of $R_{wp} = R_e$. R_F^2 = R-structure factor based on observed and calculated structure-amplitudes = $\Sigma|(F_o^{1/2} - F_c^{1/2})|\} / \Sigma F_o^{1/2}$; $\chi^2 = [R_{wp} / R_e]$, where $R_e = [(N - P)/ (\Sigma w I_o^2)]^{1/2}$, N being the number of observations (data points ≈ 2115) and P being the number of variables [a scale factor, background (24), profile (4), and structural parameters (10); total = 39]; $N_{obs.}$ = number of observed reflections = 48.

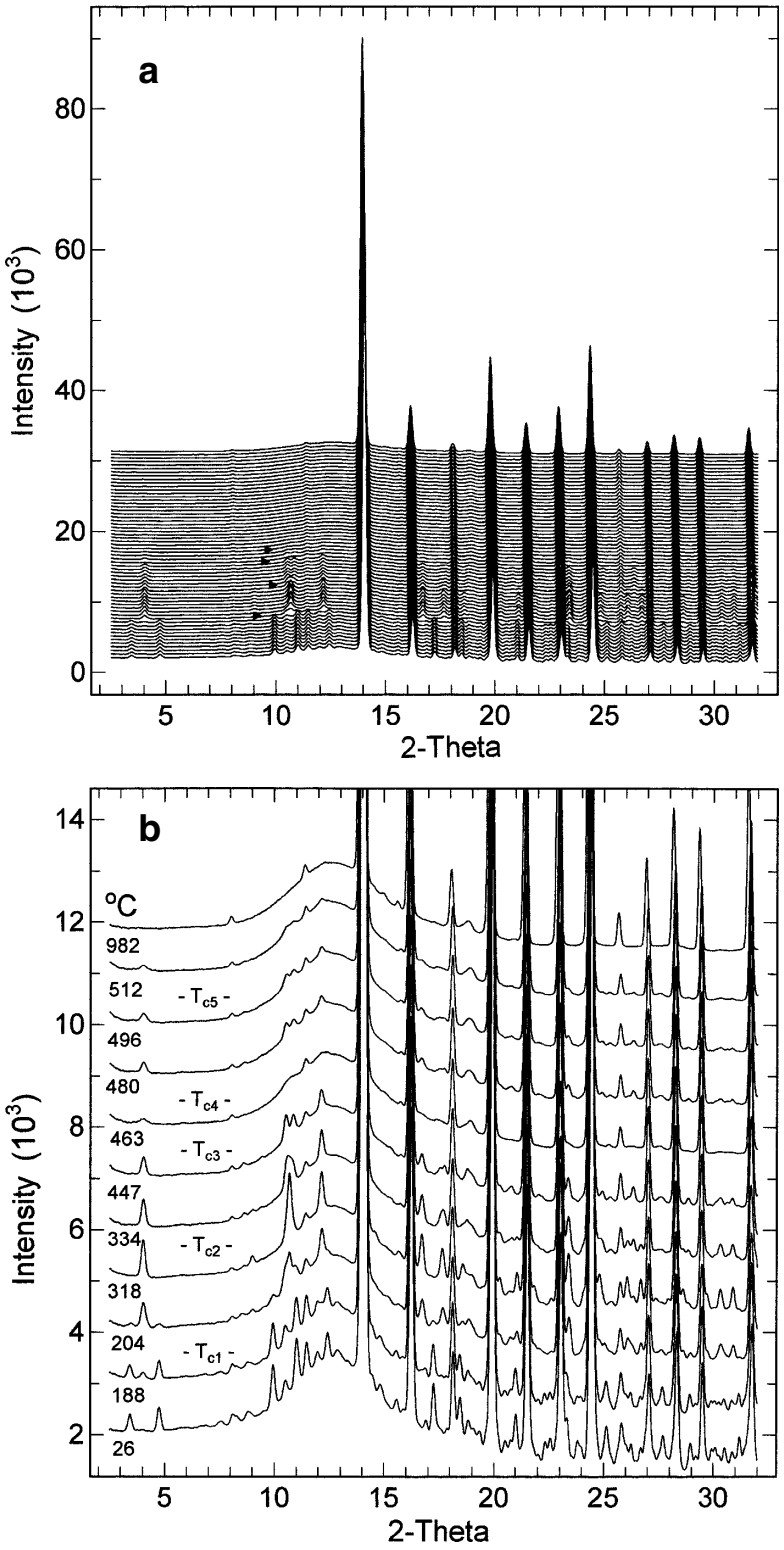
a
Intensity (10^3)
2-Theta
b
°C
982
512
- Tc5 -
496
480
- Tc4 -
463
- Tc3 -
447
334
- Tc2 -
318
204
- Tc1 -
188
26
Intensity (10^3)
2-Theta

TABLE 2. POSITIONAL AND ISOTROPIC* DISPLACEMENT-PARAMETERS ($U \times 100$ Å^2) AT VARIOUS TEMPERATURES FOR CUBIC CHROMATE ALUMINATE SODALITE

Atom§/T		463°C	512	561	626	674	723	771	820	869	901	933	982°C
Al§	U	1.17(3)	1.13(4)	1.22(3)	1.26(3)	1.25(3)	1.29(4)	1.28(3)	1.32(3)	1.32(3)	1.32(3)	1.30(4)	1.30(4)
O	x	0.1591(2)	0.1591(2)	0.1592(2)	0.1592(2)	0.1591(2)	0.1590(2)	0.1591(2)	0.1590(2)	0.1590(2)	0.1590(1)	0.1591(2)	0.1590(2)
	z	0.4560(3)	0.4561(3)	0.4565(3)	0.4566(3)	0.4567(3)	0.4568(3)	0.4571(3)	0.4573(3)	0.4575(3)	0.4575(3)	0.4576(3)	0.4579(3)
	U	5.69(6)	5.65(6)	5.83(6)	5.81(6)	5.75(6)	5.74(6)	5.65(6)	5.61(6)	5.56(6)	5.52(6)	5.50(6)	5.42(6)
Ca	x	0.2166(1)	0.2166(1)	0.2166(1)	0.2167(1)	0.2169(1)	0.2170(1)	0.2173(1)	0.2175(1)	0.2177(1)	0.2178(1)	0.2179(1)	0.2181(1)
	U	6.84(5)	6.82(5)	6.94(5)	6.87(4)	6.81(5)	6.77(5)	6.67(5)	6.63(4)	6.57(4)	6.54(4)	6.50(5)	6.43(5)
Cr	U	5.20(6)	5.16(6)	5.27(6)	5.31(6)	5.40(6)	5.52(6)	5.72(6)	5.81(6)	5.90(6)	6.01(6)	6.10(6)	6.19(7)
*O_{Cr}	x	0.1271(3)	0.1269(3)	0.1267(3)	0.1268(3)	0.1265(3)	0.1263(3)	0.1262(3)	0.1261(3)	0.1257(3)	0.1254(3)	0.1253(3)	0.1247(3)
	z	-0.0338(6)	-0.0340(6)	-0.0339(6)	-0.0331(6)	-0.0323(6)	-0.0316(6)	-0.0308(6)	-0.0306(6)	-0.0303(6)	-0.0300(6)	-0.0297(7)	-0.0296(7)

§ Al is at (¼, ½, 0); Ca at (x, x, x); Cr at (0, 0, 0), O and O_{Cr} at (x, x, z). *Constraints: $U_{Cr} = U_{OCr}$.

TABLE 3. BOND DISTANCE (Å) AND ANGLE (°) AT VARIOUS TEMPERATURES FOR CUBIC CHROMATE ALUMINATE SODALITE

Bond or angle/T		463°C	512	561	626	674	723	771	820	869	901	933	982°C
Al – O	4×	1.738(1)	1.738(1)	1.738(1)	1.738(1)	1.738(1)	1.739(1)	1.738(1)	1.739(1)	1.739(1)	1.739(1)	1.739(1)	1.739(1)
O – Al – O	4×	103.5(1)	103.5(1)	103.4(1)	103.5(1)	103.5(1)	103.5(1)	103.5(1)	103.5(1)	103.5(1)	103.5(1)	103.5(1)	103.6(1)
	2×	122.3(1)	122.3(1)	122.4(1)	122.3(1)	122.3(1)	122.2(1)	122.2(1)	122.2(1)	122.1(1)	122.1(1)	122.2(1)	122.1(1)
<O – Al – O>		**109.7(4)**	**109.7(4)**	**109.7(4)**	**109.7(4)**	**109.7(4)**	**109.7(4)**	**109.7(4)**	**109.7(3)**	**109.7(3)**	**109.7(3)**	**109.7(4)**	**109.7(4)**
Al – O – Al		139.5(2)	139.5(2)	139.6(2)	139.6(2)	139.7(2)	139.8(2)	139.9(2)	140.0(2)	140.1(2)	140.1(1)	140.1(2)	140.3(2)
Ca – O	3×	2.332(3)	2.333(3)	2.336(3)	2.338(3)	2.339(3)	2.340(3)	2.342(3)	2.344(2)	2.346(2)	2.346(2)	2.346(3)	2.349(3)
	3×	2.899(2)	2.898(2)	2.896(2)	2.897(2)	2.897(2)	2.898(2)	2.896(2)	2.896(2)	2.896(2)	2.896(2)	2.896(2)	2.896(2)
Ca – O_{Cr}	3×	2.588(6)	2.591(6)	2.593(6)	2.587(6)	2.586(6)	2.583(6)	2.583(6)	2.585(6)	2.589(6)	2.590(6)	2.591(7)	2.597(7)
<Ca – O>		**2.606(1)**	**2.607(1)**	**2.608(1)**	**2.607(1)**	**2.607(1)**	**2.607(1)**	**2.607(1)**	**2.608(1)**	**2.610(1)**	**2.611(1)**	**2.611(1)**	**2.614(1)**
Cr – O_{Cr}	12×	1.686(4)	1.685(4)	1.682(4)	1.683(4)	1.678(4)	1.675(4)	1.674(4)	1.672(4)	1.667(4)	1.663(4)	1.661(4)	1.655(4)
O_{Cr} – Cr – O_{Cr}	4×	118.88(4)	118.86(4)	118.86(4)	118.92(4)	118.96(4)	119.00(4)	119.05(4)	119.06(4)	119.07(4)	119.09(4)	119.10(4)	119.10(4)
	2×	91.96(7)	91.98(7)	91.98(7)	91.89(7)	91.81(7)	91.74(7)	91.66(7)	91.64(7)	91.62(7)	91.59(7)	91.57(7)	91.56(7)
<O_{Cr} – Cr – O_{Cr}>		**109.91(2)**	**109.90(2)**	**109.90(2)**	**109.91(2)**	**109.91(2)**	**109.91(2)**	**109.92(2)**	**109.92(2)**	**109.92(2)**	**109.92(2)**	**109.92(2)**	**109.92(2)**
* φ_{Al}		15.46	15.41	15.29	15.27	15.22	15.20	15.11	15.04	14.98	14.96	14.94	14.84

*φ is calculated from geometry of the structure, so no errors are given.

denoted T_{c1} to T_{c5}. A summary of the phase transitions is given in Table 4. Visually, the trace at 463°C is close to being cubic, but because it is sandwiched by tetragonal phases at higher and lower temperatures, the phase at 463°C is interpreted as a modulated-cubic phase. The cubic phase occurs at and above 512°C and the space

FIG. 2. Phase transitions in chromate aluminate sodalite with temperature. (a) The diffraction traces are from 26 to 982°C in intervals of 17°C. The arrowheads point out several transitions. (b) Selected traces at different temperatures point out five transitions.

TABLE 4. PHASE TRANSITIONS IN CHROMATE ALUMINATE SODALITE WITH INCREASING TEMPERATURE

Crystal System	Interval	Transition§ T_c	Space Group
Orthorhombic	26 – 188°C		*Aba*2?
		T_{c1} = 196°C	
Tetragonal 1	204 – 318°C		$P\bar{4}c2$
		T_{c2} = 326°C	
Tetragonal 2	334 – 447°C		$P\bar{4}c2$
		T_{c3} = 455°C	
Cubic (modulated)	463°C		Pseudo-cubic, $I\bar{4}3m$
		T_{c4} = 472°C	
Tetragonal 3	480 – 496°C		$P\bar{4}c2$
		T_{c5} = 504°C	
Cubic	512 – 982°C		$I\bar{4}3m$

§ Transition temperatures of 159, 180, 282, and 337°C were reported by Melzer & Depmeier (1996).

group is $I\bar{4}3m$ (Fig. 2b). The satellite reflections in the modulated cubic chromate aluminate sodalite phase are very weak and were unobserved by synchrotron X-ray diffraction, but they were observed in SAED patterns (Hassan 1996d). Therefore, the modulated-cubic phase at 463°C was refined in space group is $I\bar{4}3m$, but without evidence to indicate a splitting of the framework O atom positions, as occurs in nosean and lazurite, to explain the origin of the satellite reflections. This may indicate a limitation of the powder-diffraction technique.

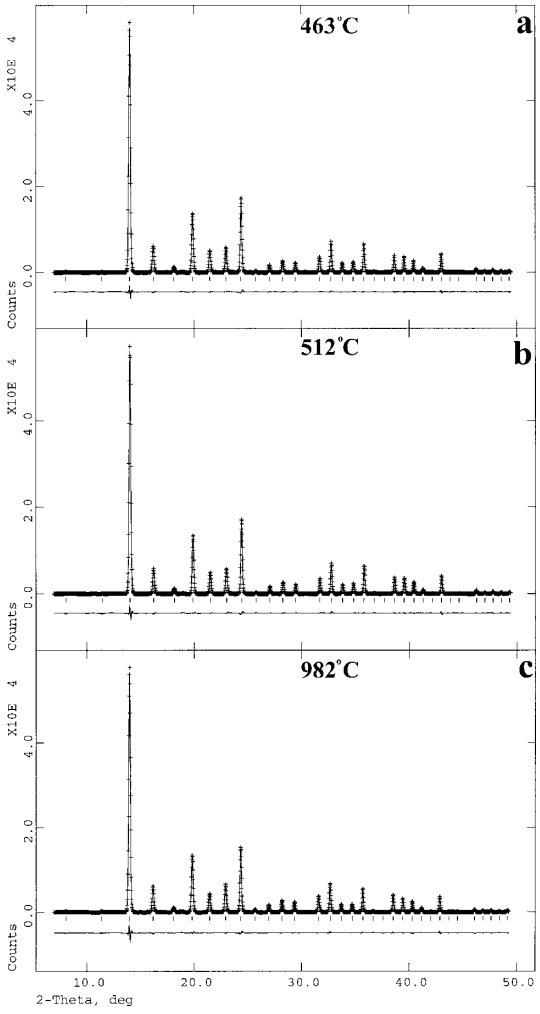

FIG. 3. Synchrotron XRD traces for chromate aluminate sodalite at: (a) 463°C, (b) 512°C and (c) 982°C, together with the calculated and difference plots from Rietveld refinements. The trace at 463°C is interpreted as a modulated cubic phase with unobservable satellite reflections; it is the only trace of this phase recorded, but it occurs in the tetragonal phase region.

Melzer & Depmeier (1996) reported four transitions for chromate aluminate sodalite: cubic above 337°C, tetragonal-2 between 337 and 282°C, tetragonal-1 between 282 and 180°C, orthorhombic-2 between 180 and 159°C, and orthorhombic-1 between 159 and 25°C. Their transition temperature at 180°C could correspond to our T_{c1} transition between our orthorhombic and tetragonal-1 phases (Table 4), but their 337°C transition temperature to the cubic phase is low compared to 504°C observed in this study. The difference in results is not easy to explain and could be related to compositions of the materials or to the experimental methods used. Unfortunately, we were unable to do a chemical analysis of our sample because it was used up, and neither could we run a differential thermal analysis (DTA). However, the structure refinements indicate that our sample is stoichiometric.

Cell parameters

Except for the modulated cubic phase at 463°C, the *a* cell parameter for cubic chromate aluminate sodalite increases linearly with temperature (Fig. 4). The data point at 463°C does not fall on the trend line for the cell parameters, which is consistent with our hypothesis that at 463°C, a separate modulated cubic phase exists. If the data point at 463°C is excluded, all the other data points fall on a straight line (Fig. 4). The unit-cell parameter for cubic chromate aluminate sodalite at 512°C obtained in this study [Table 1; a = 9.22293(6) Å] is

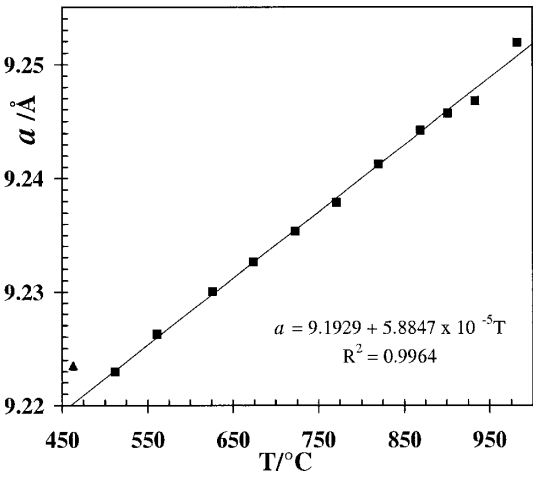

FIG. 4. The thermal-expansion curve for cubic chromate aluminate sodalite. The equation for the least-squares fit to the data is given as an insert. The data point for the modulated cubic phase at 463°C is shown as a solid triangle and is excluded from the least-squares fit. Error bars are smaller than the symbols.

slightly different from that obtained at 427°C [a = 9.2211(5) Å] by Melzer & Depmeier (1996) and may be related to the difference in temperatures. The a parameter expansion between 512 and 982°C is given by the least-squares fit (all T in °C): $a = 9.1929 + 5.8847 \times 10^{-5}$T (Fig. 4). The coefficient of linear thermal expansion, $\alpha_a = (da/dT)(1/a)$, calculated from the above equation, varies between 6.381×10^{-6} °C^{-1} at 512°C and 6.361×10^{-6} °C^{-1} at 982°C. The volume expansion between 512 and 982°C is given by the least-squares fit: $V = 777.4455 + 1.4341 \times 10^{-2}$T. The coefficient of volume thermal expansion, α_V, varies between 1.828×10^{-5}° C^{-1} at 512°C and 1.811×10^{-5}° C^{-1} at 982°C. The percent change in volume between 512 and 982°C is 0.9(1)%.

The percent change in volume in sodalite, $Na_8[Al_6Si_6O_{24}]Cl_2$, between 28 and 982°C is 4.8(2)% (Hassan *et al*. 2004a), which is much larger than that in chromate aluminate sodalite. The higher net charge, $[Ca_4{\bullet}CrO_4]^{6+}$ in chromate aluminate sodalite, compared to $[Na_4{\bullet}Cl]^{4+}$ clusters in sodalite, limits the expansion in cubic chromate aluminate sodalite. Furthermore, the large size of $[Ca_4{\bullet}CrO_4]^{6+}$ in chromate aluminate sodalite compared to $[Na_4{\bullet}Cl]^{4+}$ clusters in sodalite affects the degree of collapse of the cages.

The percent change in volume between 33 and 1035°C is 1.6(1)% in danalite, $Fe_8[Be_6Si_6O_{24}]S_2$ (Antao *et al.* 2003). This volume change is small because of the highly charged $[Fe_4{\bullet}S]^{6+}$ clusters. These highly charged clusters bond strongly to the framework O, and limit the extent of thermal expansion. Moreover, danalite is in a highly collapsed state (*e.g.*, φ_{Si} = 32.11° at 33°C) compared to sodalite (φ_{Si} = 23.6° at 28°C), or chromate aluminate sodalite (φ_{Al} = 15.41° at 512°C), as judged from these angles of rotation of the framework tetrahedra. Although these data are compared for different temperatures, the fact that the expansion of chromate aluminate sodalite is quite small allows the degree of collapse to be correlated with the size of the cage clusters. However, the framework T atoms should also be to be taken into account for completeness. The Si–O and Be–O bond lengths are similar (about 1.630 Å) and shorter than the Al–O distance (about 1.738 Å). The size of the various clusters can be judged from the following bond-distances: Fe–S = 2.413 Å in danalite, Na–Cl = 2.716 Å in sodalite, and Ca–Cr = 3.460 Å in chromate aluminate sodalite. Therefore, the size of the clusters is mainly responsible for the degree of collapse in the different structures. The larger the cage clusters, the less is the degree of collapse.

Structure and framework of cubic chromate aluminate sodalite

The general structural features of chromate aluminate sodalite have been described, and the structure obtained at 982°C is shown (Fig. 1). This structure is quite similar to that obtained by Melzer & Depmeier (1996). The Al atom is on the 12(d) site in space group $I\bar{4}3m$, and the four equivalent Al–O distances are 1.738(1) Å at 463°C (Table 3).

The interstitial Ca^{2+} cations occupy an 8(c) position on the 3-fold axes and are coordinated by three O atoms that have short bonds and three O' atoms that are further away. The framework oxygen atoms O and O' are related by symmetry, as they are on the 24(g) site. The coordination of the Ca^{2+} cation is completed by O_{Cr} atoms of the CrO_4^{2-} group, which is disordered (Table 3). The O_{Cr} atom is disordered on a 24(g) site, and the Cr atom occurs on the 2(a) site.

The framework of chromate aluminate sodalite consists of corner-linked AlO_4 tetrahedra. Between 463 and 982°C, the Al–O distance is nearly constant with temperature (Fig. 5a). In sodalite, between 28 and 982°C, the T–O distance also is constant (Hassan *et al*. 2004a).

In the framework tetrahedra, the four equivalent O–T–O angles and the two equivalent O–T–O angles are constant with temperature, so the average <O–T–O> is constant (Table 3, Fig. 5b). The Al–O–Al bridging angle increases slightly with temperature (Fig. 5b); from 463 to 982°C, it increases from 139.5(2) to about 140.3(2)°, a difference of 0.8(2)° (Table 3). In sodalite, from 28 to 982°C, the Al–O–Si angle increases by 5.06(2)° (Hassan *et al*. 2004a).

The CrO_4^{2-} group in a cage occupies disordered positions, which leads to an irregular geometry for the tetrahedral CrO_4^{2-} group. The Cr–O_{Cr} distance is 1.686(4) Å at 463°C, and it decreases slightly with temperature (Table 3, Fig. 5a).

The cage contains interstitial Ca^{2+} cations that are bonded to three framework O atoms at a short distance of 2.332(3) Å and three more (symmetry-equivalent) framework O' atoms at a distance of 2.899(2) Å at 463°C (Table 3). In addition, the Ca atom is bonded to the disordered O_{Cr} oxygen atoms of the CrO_4^{2-} group. The Ca–O distances are all nearly constant with temperature (Fig. 5a).

The variation of the isotropic displacement parameters, U, for all the atoms in cubic chromate aluminate sodalite is shown (Fig. 5c). These displacement parameters have normal values.

The mechanism of thermal expansion for chromate aluminate sodalite

The geometrical model for the thermal expansion of sodalite (Hassan & Grundy 1984) is combined with the present results to describe the thermal behavior of cubic chromate aluminate sodalite. In the thermal expansion, the cage clusters may expand and force the interstitial Ca cations toward the plane of the six-membered ring, which causes the framework tetrahedra to rotate. The AlO_4 tetrahedra rotate through an angle φ_{Al} (Fig. 1), which is calculated at different temperatures using equation 8 of Hassan & Grundy (1984), and its variation with temperature is shown (Fig. 6a). Between 463 and 982°C,

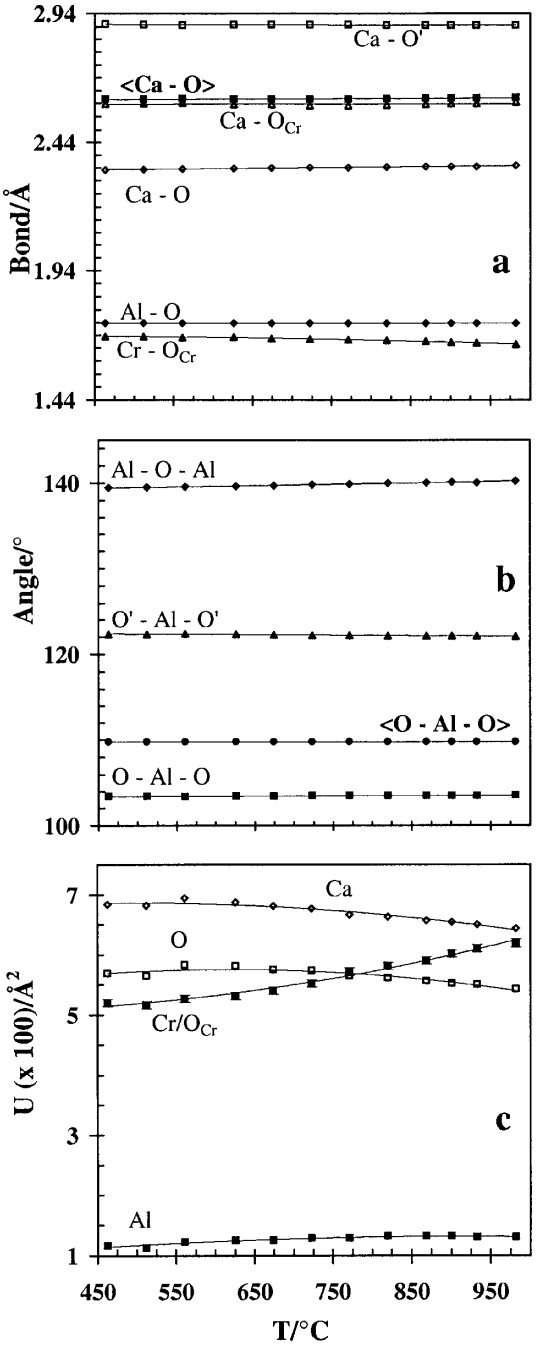

FIG. 5. (a) Variation of the Al–O, Ca–O, and Cr–O_{Cr} bond distances with temperature. (b) Variation of the Al–O–Al bridging angle and of bond angles in the framework AlO_4 tetrahedra with temperature. (c) Variation of the isotropic displacement parameters, *U*, with temperature. Error bars are not seen if smaller than the symbols. The data points for the modulated cubic phase at 463°C are included in the graphs.

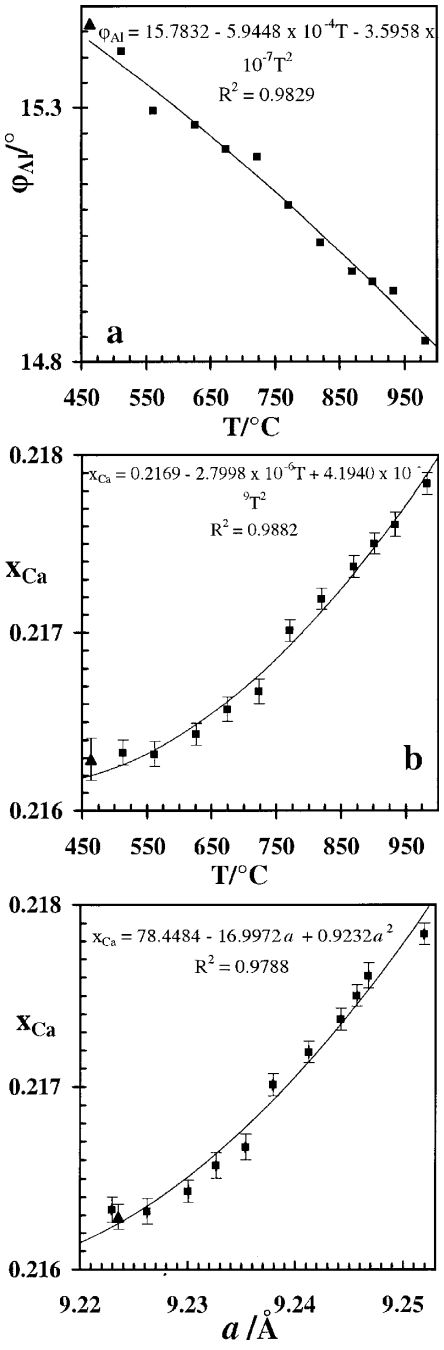

FIG. 6. (a) Variation of the angle of rotation, ϕ_{Al}, of the AlO_4 tetrahedron with temperature (see Fig. 1). Variation of the atom coordinate of the interstitial Ca atom, x_{Ca}, (b) with temperature, and (c) with the *a* cell parameter. The data points for the modulated cubic phase at 463°C are shown as solid triangles and are excluded from the least-squares fit.

φ_{Al} changes from 15.46 to 14.84°, a difference of 0.6°. Simultaneously, the Al–O–Al bridging angle changes from 139.5(2) to 140.3(2)°, a difference of 0.8(2)°. In sodalite, between 28 and 982°C, φ_{Al} decreases from 22.1 to 16.9°, a difference of 5.2°, whereas the φ_{Si} decreases from 23.6 to 18.0°, a difference of 5.6° and the Al–O–Si angle increases by 5.06(2)° (Hassan *et al*. 2004a). In danalite, φ_{Be} and φ_{Si} decrease by about 0.7° from 33 to 926°C (Antao *et al*. 2003). At 512°C, cubic chromate aluminate sodalite (φ_{Al} = 15.41°) is in a less collapsed state than that at 28°C in sodalite (φ_{Si} = 23.6°, φ_{Al} = 22.1°), as judged from the angles of rotation. However, with temperature, the degree of rotation of the tetrahedra in cubic chromate aluminate sodalite (0.6°) and danalite (0.7°) are quite small compared to that in sodalite (5.2°).

As the structure expands, the interstitial Ca^{2+} cations move along <111> toward the plane of the six-membered rings and cause the tetrahedra to rotate in aluminate sodalite. The change in the coordinate *x* of the interstitial Ca^{2+} cation with the *a* cell parameter and temperature is given in Figures 6b and 6c. From 463 to 982°C, the extent of migration of the Ca^{2+} cation is quite small. If the interstitial Ca^{2+} cation reaches (¼, ¼, ¼), then it is midway between the center and a corner of the cell and approximately in the plane of the six-membered rings, and the expansion rate is expected to decrease. However, the interstitial Ca^{2+} cations are far from (¼, ¼, ¼) in cubic chromate aluminate sodalite at 982°C. The coordination of the interstitial Ca^{2+} cation and its location with respect to a six-membered ring are shown for the structure at 982°C (Fig. 7). The Ca^{2+} cation is located nearly in the plane of the three O' framework atoms, so movement of the Ca^{2+} cation out of this plane will cause longer Ca–O' bonds, instead of shorter bonds that usually occur where the cation is migrating toward the above plane. The location of the Ca^{2+} cations in this plane is one reason why the expansion is small in chromate aluminate sodalite. A similar location of the interstitial cation occurs in haüyne and causes an abrupt change in the expansion (Hassan *et al*. 2004b). In the case of chromate aluminate sodalite, the Ca^{2+} cations are located in the plane of the three O' atoms throughout the temperature range studied. In danalite, the Fe^{2+} cations are not in the plane of the three O1' atoms, yet the expansion is quite small compared to that in sodalite. Therefore, in addition to the location of the cations in the plane of the three O1' atoms as in chromate aluminate sodalite, the highly charged clusters ($[Fe_4•S]^{6+}$ in danalite, and $[Ca_4•CrO_4]^{6+}$ in chromate aluminate

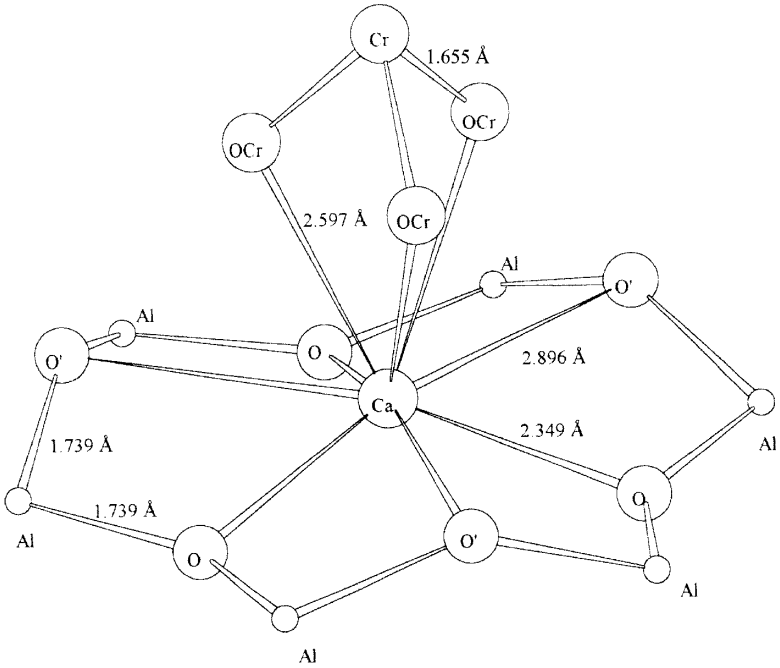

FIG. 7. Coordination of an interstitial Ca^{2+} cation in chromate aluminate sodalite at 982°C. A six-membered ring is shown. The O' atoms do not form typical Ca–O bonds, as they are too long. The Ca atom is nearly in the plane of the three O' atoms. The displacement parameters are shown to scale at the 20% probability level.

sodalite, compared to $[Na_4•Cl]^{4+}$ in sodalite) must resist the expansions. The highly charged clusters bond strongly to the framework O atoms, and this limits the rotation of the framework AlO_4 tetrahedra. Therefore, the charge of the clusters is related to the degree of rotation of the tetrahedra, whereas the size of the clusters is related to the degree of collapse of the structure.

Acknowledgements

This research was carried out in part at the National Synchrotron Light Source, Brookhaven National Laboratory (BNL), which is supported by the U.S. Department of Energy, Division of Materials Sciences and Division of Chemical Sciences, under Contract No. DE–AC02–98CH10886. We thank Jonathan C. Hanson of BNL for his help in performing the synchrotron experiments and we also thank the referees, S. Latturner, R.F. Martin, and an anonymous reviewer, for useful comments on this paper. This study was supported by a NSF grant EAR–0125094 to J.B.P.

References

Antao, S.M., Hassan, I. & Parise, J.B. (2003): The structure of danalite at high temperature obtained from synchrotron radiation and Rietveld refinements. *Can. Mineral.* **41**, 1413-1422.

_____, _____ & _____ (2004): Tugtupite: high temperature structures obtained from in situ synchrotron radiation and Rietveld refinements. *Am. Mineral.* **89**, 492-497.

Hammersley, J. (1996): *Fit2d User Manual*. ESRF Publication, Grenoble, France.

Hassan, I. (1996a): Direct observation of phase transitions in aluminate sodalite, $Ca_8[Al_{12}O_{24}](CrO_4)_2$. *Am. Mineral.* **81**, 1375-1379.

_____ (1996b): Two-dimensional periodic antiphase boundaries in a synthetic aluminate sodalite, $Ca_8[Al_{12}O_{24}](CrO_4)_2$. *Can. Mineral.* **34**, 1031-1038.

_____ (1996c): Aluminate sodalite, $Ca_8(Al_{12}O_{24})(CrO_4)_2$, with tetragonal and orthorhombic superstructures. *Eur. J. Mineral.* **8**, 477-486.

_____ (1996d): Structural modulations in a pseudo-cubic aluminate sodalite, $Ca_8[Al_{12}O_{24}](CrO_4)_2$. *Z. Kristallogr.* **211**, 228-233.

_____ (1996e): Twinning in aluminate sodalite, $Ca_8[Al_{12}O_{24}](CrO_4)_2$. *Mineral. Mag.* **60**, 617-622.

_____ (2000): Transmission electron microscopy and differential thermal studies of lazurite polymorphs. *Am. Mineral.* **85**, 1383-1389.

_____, Antao, S.M. & Parise, J.B. (2004a): Sodalite: high temperature structures obtained from synchrotron radiation and Rietveld refinements. *Am. Mineral.* **89**, 359-364.

_____, _____ & _____ (2004b): Haüyne: phase transition and high temperature structures obtained from synchrotron radiation and Rietveld refinements. *Mineral. Mag.* **68**, 499-513.

_____ & Buseck, P.R. (1989a): Incommensurate-modulated structure of nosean, a sodalite-group mineral. *Am. Mineral.* **74**, 394-410.

_____ & _____ (1989b): Cluster ordering and antiphase domain boundaries in haüyne. *Can. Mineral.* **27**, 173-180.

_____ & Grundy, H.D. (1984): The crystal structures of sodalite-group minerals. *Acta Crystallogr.* **B40**, 6-13.

_____, Peterson, R.C. & Grundy, H.D. (1985): The crystal structure of lazurite, ideally $Na_6Ca_2(Al_6Si_6O_{24})S_2$, a member of the sodalite group. *Acta Crystallogr.* **C41**, 827-832.

Henderson, C.M.B. & Taylor, D. (1978): The thermal expansion of synthetic aluminate-sodalites, $M_8(AR_6Si_6O_{24})X_2$. *Phys. Chem. Minerals* **2**, 337-347.

Larson, A.C. & Von Dreele, R.B. (2000): General Structure Analysis System (*GSAS*). *Los Alamos Nat. Lab., Rep.* **LAUR 86-748**.

Melzer, R. & Depmeier, W. (1996): A structural study of aluminate sodalite, $Ca_8[Al_{12}O_{24}](CrO_4)_2$. *Cryst. Res. Technol.* **31**, 459-467.

Morimoto, N. (1978): Incommensurate superstructures in transformation of minerals. *Recent Prog. Nat. Sci. Japan* **3**, 183-206.

Saalfeld, H. (1961): Strukturbesonderheiten des Hauyngitters. *Z. Kristallogr.* **115**, 132-140.

Schulz, H. (1970): Struktur und Überstrukturuntersuchungen an Nosean-einkristallen. *Z. Kristallogr.* **131**, 114-138.

Taylor, D. (1968): The thermal expansion of sodalite group of minerals. *Mineral. Mag.* **36**, 761-769.

Toby, B.H. (2001): EXPGUI, a graphical user interface for GSAS. *J. Appl. Crystallogr.* **34**, 210-213.

Tsuchiya, N. & Takéuchi, Y. (1985): Fine texture of hauyne having a modulated structure. *Z. Kristallogr.* **173**, 273-281.

Van Smaalen, S., Dinnebier, R., Katzke, H. & Depmeier, W. (1997): Structural characterization of the high-temperature phase transitions in $Ca_8[Al_{12}O_{24}](MoO_4)_2$ aluminate sodalite using X-ray powder diffraction. *J. Solid State Chem.* **129**, 130-143.

Received January 9, 2004, revised manuscript accepted June 28, 2004.